ISSN 1028-334X, Doklady Earth Sciences, 2006, Vol. 410, No. 7, pp. 1096–1100. © Pleiades Publishing, Inc., 2006.
Original Russian Text © A.A. Krasnobaev, G.B. Fershtater, F. Bea, P. Montero, 2006, published in Doklady Akademii Nauk, 2006, Vol. 410, No. 2, pp. 244–249.

GEOCHEMISTRY

Polygenous Zircons in the Adui Batholith (Middle Urals)

A. A. Krasnobaev[a], G. B. Fershtater[a], F. Bea[b], and P. Montero[b]

Presented by Academician O.A. Bogatikov August 28, 2005

Received August 9, 2005

DOI: 10.1134/S1028334X0607021X

The Adui Massif, the largest batholith in the northwestern paleocontinental zone of the Urals, is highly similar to the northern Murzinka Massif. These batholiths probably make up a single massif (Fig. 1). The Adui Batholith is composed of granites of different compositions and ages. Biotite and two-mica (orthoclase and microcline) granites and younger adamellites prevail among the granites. These rocks are intruded by numerous pegmatite and aplite veins.

Datings of the Adui granite (AG) by the Rb–Sr, K–Ar, Re–Os, and U–Pb monazite methods have yielded an age of 250–265 Ma, which is consistent with the age parameters of the Murzinka Massif [1]. An overview of these investigations is presented in [2, 3]. Interest in the dating of the Murzinka Massif was revived by polygenous zircon data based on the Kober Pb–Pb and laser ablation ICP-MS (hereafter, LA-ICP-MS) methods, which make it possible to date separate crystals or their parts.

The detailed investigation of two AG zircon samples yielded fundamentally new data that need special analysis regarding the issue formulated above.

Separate zircon grains in polished sections were dated and analyzed for 25 rare elements at the University of Grenada. The LA-ICP-MS analysis was carried out with a Mercantek 213-nm laser (beam diameter 55–60 μm) equipped with Agilent 7500s spectrometer in a helium atmosphere. The sample was raised for 5 μm every 20 s in order to maintain the constancy of the laser beam. The NIST-610 glass containing ~0.450 ppm of each element was used as the standard. Each run was started and terminated with the analysis of the standard. In addition, analysis of the standard was repeated after every four datings and eight composition measurements in order to correct the drift. Zirconium and silicon were used as internal standards. The results were processed with the Bea software package. Accuracy of measurements was ±1% for the $^{238}U/^{208}Pb$ ratio and ~3% for absolute concentrations of REE and other rare elements. Pb isotope ratios in the NIST-610 glass used for the U–Pb calibration were determined at the University of Grenada. Mass fractionation was measured and corrected by the $^{203}Tl/^{205}Tl$ ratio. Accuracy of U–Pb datings was checked by the ion probe analysis of zircon in the Almohalla orthogneiss (Central Spain) by the Kober ^{207}Pb–^{206}Pb method. The Almohalla zircon has a stable age of 543 ± 3 Ma.

Zircons were extracted from granites (sample K1252) and adamellites (sample K1253). Their compositions are presented in Table 1.

The Adui granite contains a polygenous zircon population (Fig. 2). In addition to the typical granitic zircons, species of problematic genesis are also present. The AG zircons in both samples can easily be subdivided into the colorless transparent (I) and yellowish brown semitransparent or opaque (II) types. Zircon I has a simple prismatic appearance related to the combination of {110}, {111}, and occasional {311} faces. Crystals of this type correspond to the characteristic late magmatic varieties enriched in U, Th, Y, P, REE, and other trace elements. The degree of metamictization of such zircons is as much as 25–30%. Zircon II is closely associated with transparent and semitransparent long-prismatic or acicular zonal crystals (with primary inclusions) of the early magmatic generation (Fig. 2, *1–4*). Such combinations of early and late zircon generations prevail in sample K1253 and occur episodically in sample K1252. The study of homogeneous short-prismatic zircon I is hampered by its high degree of idiomorphism and roundedness related to corrosion or abrasion (Fig. 2, *5–7*). This type of zircon is abundant in sample K1252 and subordinate in sample K1253. Zircon I occurs not only as separate crystals, but also as nuclei in zircon II (Fig. 2, *8–10*). Therefore, we can assume that zircon I in the AG is a xenogenic formation.

[a] *Institute of Geology and Geochemistry, Ural Division, Russian Academy of Sciences, Pochtovyi per. 7, Yekaterinburg, 620151 Russia*
e-mail: krasnobaev@igg.uran.ru
[b] *Universidad de Granada, Fuenfanueva s/n, 18002, Granada, Spain*
e-mail:mailfbea@goliat.ugr.es

This is also suggested by the fact that zircon I includes relicts of deformation structures that predated the overgrowth of zircon II (Fig. 2, *11*). Diaphthoresis of the AG is reflected in the crushing and metasomatic reworking of both zircons I and II (Fig. 2, *12*).

Cathodoluminescence properties of the studied zircons (Fig. 2, *13–20*) made it possible to refine their optical data. Zircon I shows an intense cathodoluminescence, while zircon II virtually lacks this property. Hence, zircons I and II are characterized by different degrees of crystallinity. In terms of cathodoluminescence, early magmatic acicular zircons can be compared with zircon II crystals (Fig. 2, *13*). Thus, the acicular crystals are genetically similar. In contrast, zircon I is observed as different varieties: (i) separate crystals without the overgrowth of zircon II (Fig. 2, *14*; cf.: *5*, *6*) and (ii) intergrowths with zircon II composed of nucleus (I) and shells (Fig. 2, *15–20*). The diversity of the nucleus–shell system is the main problem in the study of zircon I crystals. They represent either xenogenous formations in the AG or a different type similar to the early long-prismatic variety (Fig. 2, *2*, *3*), i.e., an early generation that predated zircon II. One can suggest the following mechanisms for the coexistence of zircons I and II in a single crystal. According to the first mechanism, the crystals can grow successively in the course of a single process of zircon formation (Fig. 2, *15*). The zonality of grains indicates the manifestation of this process since the moment of crystal nucleation (Fig. 2, *14, 15*). The second (more intricate) mechanism takes into account all the preceding processes: dissolution of zircon I crystals (Fig. 2, *16*), as well as their dissolution or abrasion (Fig. 2, *17, 18*), brittle deformation, and subsequent dissolution (Fig. 2, *19, 20*). Such features testify to the detrital (xenogenous) nature of some zircon I crystals. This scenario of the formation of zircon II crystals is evident from crystal *20* (Fig. 2, cf.: *11*), which was initially divided by a crack into two parts and then amalgamated by the subsequent overgrowth of zircon II into a single system.

The data presented above suggest that zircon I crystals are xenogenous formations. They significantly differ from the early long-prismatic crystals that characterize the standard conditions of granitic magmatism.

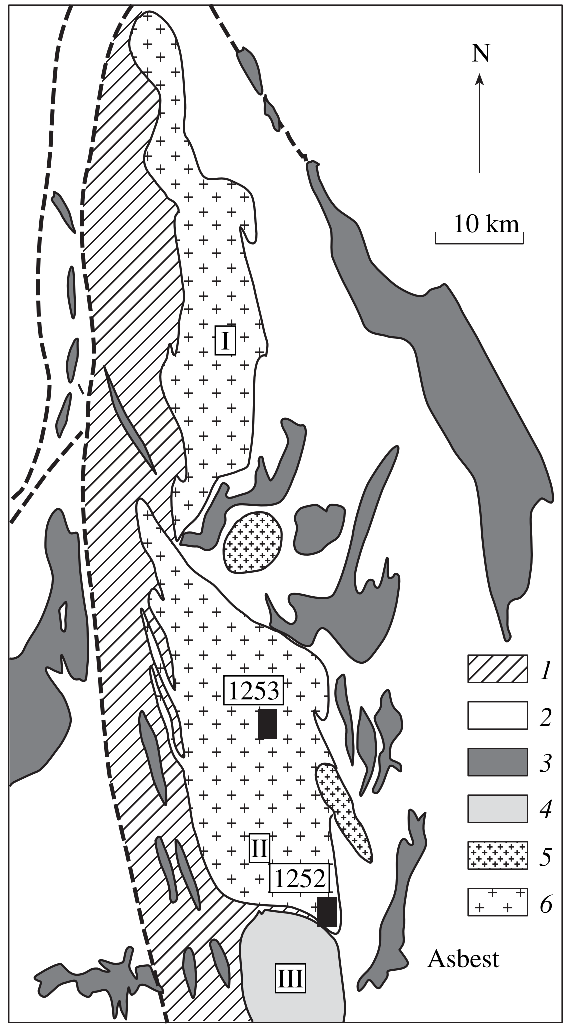

Fig. 1. Schematic geological map of the Adui Batholith area. (*1*) Murzinka metamorphic complex; (*2*) Paleozoic volcanosedimentary rocks; (*3*) serpentinites; (*4*) tonalites, granodiorites, and migmatites of the Kamensk Massif (III); (*5*) monzodiorite–granite massifs; (*6*) granites of the (I) Murzinka and (II) Adui massifs.

The LA analysis points on the crystal were carefully chosen to avoid the overlapping of materials of zircons I and II. We carried out 38 point analyses of 21 crystals. Table 2 shows U, Th, and Pb contents, as well as Zr/Hf

Table 1. Chemical compositions of rocks, from which zircons were extracted, wt %

Sample no.	SiO_2	TiO_2	Al_2O_3	Fe_2O_3	FeO	MnO	MgO	CaO	K_2O	Na_2O	P_2O_5	L.O.I.	Total
K1252	73.69	0.23	13.74	0.10	1.22	0.02	0.25	1.26	4.79	3.73	0.05	0.38	99.46
K1253	71.42	0.47	14.16	0.70	1.87	0.02	0.76	1.66	4.10	4.00	0.14	0.30	99.60

Note: (K1252) 5 km west of the town of Asbest, medium-grained myrmekitic orthoclase–perthite granite with biotite and minor muscovite (major variety); (K1253) 71 km away along the Yekaterinburg–Rezh road, medium-grained porphyric biotite adamellite with laths of zonal plagioclase and orthoclase (intrudes K1252 granites).

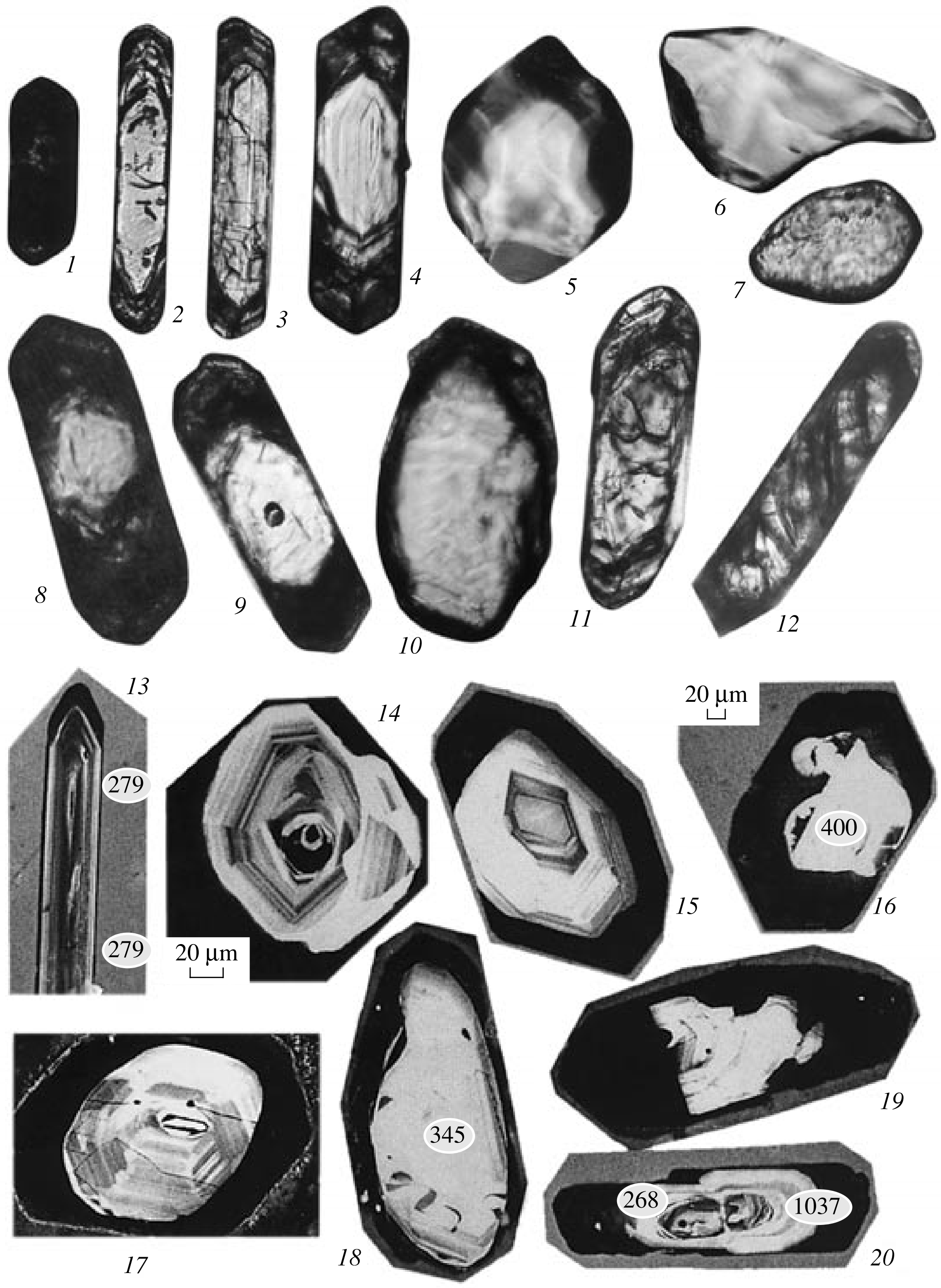

Fig. 2. Optical (*1–12*) and cathodoluminescence (*13–20*) images of zircons from the Adui Massif. Gray circles show the LA analysis points. Numbers in circles designate age, Ma. See the text for other explanations.

and Pb isotope ratios, determined for nine crystals. Other crystals are characterized by similar parameters.

The discreteness of ontological features of zircons is confirmed by their compositional variations. Long-prismatic crystals (Fig. 2, *13*) from different areas are similar in composition and age (Table 2, crystals *14* and *20*), suggesting their formation during a short time interval of the AG evolution.

Zircons I and II have the most contrasting compositions (Table 2, Fig. 3). In zircon I, the U content variation range is 200–600 ppm (in rare cases, up to 140 and 870 ppm). In zircon II, the variation range increases to

Table 2. Composition and age of zircons from granitoids of the Adui Massif

Grain no.	Content, ppm			Zr/Hf	Age based on					Coefficient of discordance (K_d)
	Pb	Th	U		$^{206}Pb/^{238}U$	$^{207}Pb/^{235}U$	$^{208}Pb/Th$	$^{207}Pb/^{206}Pb$	$^{206}Pb/^{238}U$ cor	
10c	8	64	140	67.6	345.8	350.9	378.8	385.1	345.3	1.01
12c	14	49	351	53.59	254.3	284.8	349.9	542.9	252.1	1.12
14c	21	392	384	49.1	284	285	283	293.3	283.9	1.00
14r	16	204	329	47.69	284.2	292.8	288.2	361.9	283.6	1.03
15c	16	186	189	55.32	403.2	441.6	536.7	646.7	400	1.10
15r	62	191	1333	42.58	292.5	351.1	523.9	759.3	288	1.20
20c	22	241	473	46.7	279.2	280.7	283.4	292.9	279.1	1.01
20r	24	261	502	46.74	279.7	282.2	281.6	302.9	279.5	1.01
24c	10	104	212	57.61	288.6	287.3	312.5	276.1	288.8	1.00
24r	159	363	3452	37.01	301.6	325.1	445.6	497.3	299.7	1.08
25c	80	89	446	43.96	1054	1158	1305.3	1358	1037.4	1.10
25r	130	135	4157	23.43	180.8	360.1	2611.3	1776	167.3	1.99
32c	17	166	368	49.69	282.6	283.9	299.1	294.7	282.6	1.00
32r	124	471	3024	23.55	238.8	445.7	707.4	1730	222.3	1.87
35c	14	192	289	41.39	285.4	284.9	296.2	281.1	285.5	1.00
35	157	527	3469	34.44	293	333.9	367.1	629.3	289.8	1.14
37c	23	100	544	40.94	270.7	302.5	367.1	556.3	268.3	1.12
37r	125	137	3310	21.31	223.3	409.2	2200	1663	208.7	1.83
43c	7	54	139	45.26	290.3	299.6	284.2	371.9	289.7	1.03
44c	8	74	158	51.25	290	315.1	314.1	505.1	288	1.09

Note: (c, r) Center and rim of zircon grain, respectively (or zircon I and II, respectively). $K_d = t^{207}Pb/^{235}Pb : t^{206}Pb/^{238}U$.

2000–6500 ppm (in rare cases, up to 15000 ppm). Such discrepancies are also observed in the distribution of Th and Zr/Hf. They are responsible for the discreteness of cathodoluminescence of zircons (e.g., weak cathodoluminescence of zircon II). Zircon II is appreciably enriched in LREE, Ta, and Nb.

The majority of zircon crystals show a positive U–Pb correlation (Fig. 3), which suggests the simultaneous formation of crystals. According to the most concordant datings (Table 2, Fig. 3), the crystals have an age of 291 ± 8 Ma. However, the central part (nucleus) of some crystals has a higher Pb/U ratio (Fig. 2, *16*, *18*, *20*; Table 2) and an older age (345, 400, and 1037 Ma, respectively). Within the isochron model framework, these crystals yield discordia (Fig. 4) at 338 ± 4.2 and 1451 ± 15 Ma (MSWD = 0.1), suggesting the participation of Precambrian substance in the AG formation. In the age–U diagram (Fig. 3), the field of such crystals is separated from the field of the majority of crystals confined to the age interval defined above. Moreover, one can distinctly see the rejuvenation of many crystals (particularly, U-rich zircons I and II), probably as a result of their metamict state. It is worth mentioning that datings older than 291 Ma are absent for the majority of zircon II grains; i.e., their late origin is rather obvious.

Thus, we can draw the following conclusions. Based on concordant zircon datings, the AG zircon age is estimated at 291 ± 8 Ma. All long-prismatic zircon crystals, all zircon II crystals, and the majority of zircon I crystals were formed at this age boundary. However, the genetic nature of zircon I does not fit the scenario of a single process. Some zircon I crystals undoubtedly represent the AG substrate with an age of no less than 1451 Ma. The involvement of such crystals in the AG evolution was accompanied by the recrystallization and resetting of their radiological system at the zero level. Only a few crystals could retain the isotope memory of their early stages.

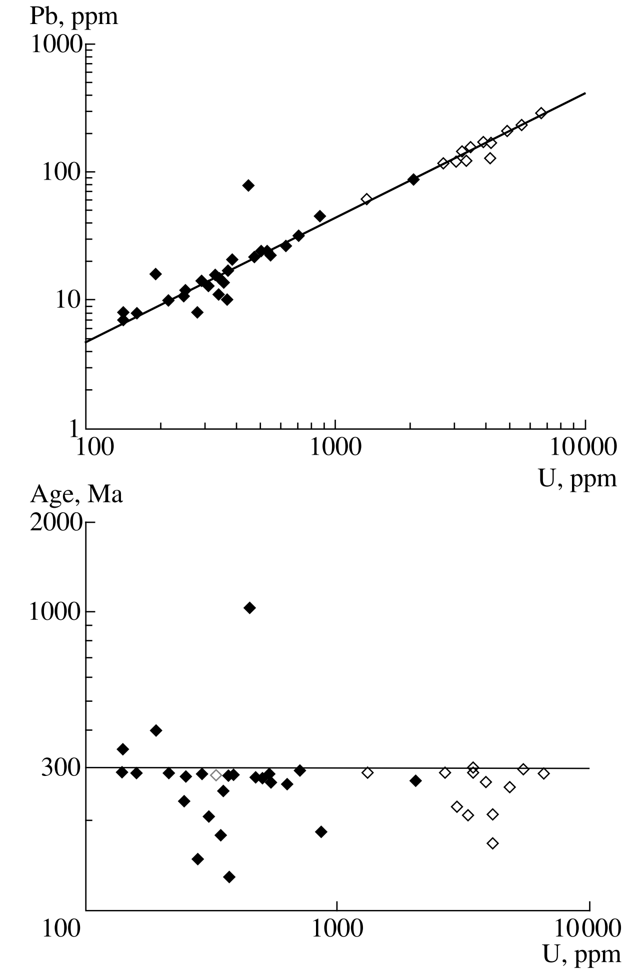

Fig. 3. U–Pb diagrams and U age of zircons from the Adui Massif. Filled diamonds designate central parts of grains; open diamonds, rims.

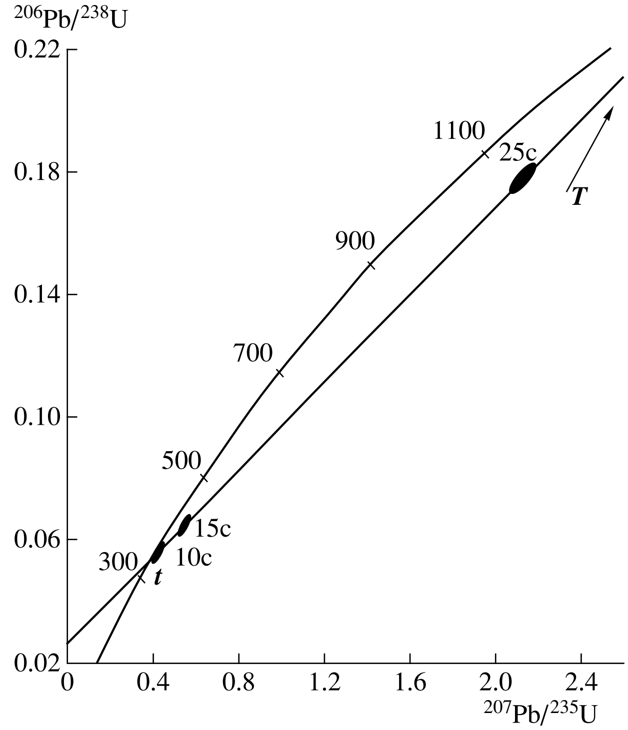

Fig. 4. $^{207}Pb/^{235}U$–$^{206}Pb/^{238}U$ diagram with discordia for grains 10c, 15c, and 25c. $t = 338 \pm 4.2$, $T = 1451 \pm 15$ Ma, MSWD = 0.1.

The major portion of the AG substrate was presumably represented by igneous rocks, such as gneisses of the Murzinka Complex (no less than 1650 Ma old [4]) and granodiorites of the Kamensk Massif (320–340 Ma) exposed south of the Adui Massif. Processes of the AG diaphthoresis recorded by some crystals (Fig. 2, *12*) were responsible for the disturbance of their isotope parameters and rejuvenation, which is particularly well manifested in crystals with a higher concentration of trace elements.

The age discrepancy revealed by the LA-ICP-MS zircon dating can be explained in the following way. The zircon crystals could retain the memory of early stages of granite formation (290 Ma), migmatization, and anatexis, which promoted not only the formation of new generations, but also the partial recrystallization (homogenization) of crystals adopted from the substrate. The appearance of zircon crystals with an age of <290 Ma and the younger K–Ar and Rb–Sr datings of 250–260 Ma are related to several magmatic stages in the later history of the Adui Batholith.

ACKNOWLEDGMENTS

This work was supported by the Russian Foundation for Basic Research (project no. 05-05-64079), the Foundation of the President of the Russian Federation for the Support of Leading Scientific Schools (project no. NSh-85.2003.5), and the Division of Earth Sciences of the Russian Academy of Sciences (program no. 7).

REFERENCES

1. P. Montero, F. Bea, A. Gerdes, et al., Tectonophysics **317**, 93 (2000).
2. V. S. Popov, V. I. Bogatov, Yu. A. Petrova, and B. V. Belyatskii, Litosfera, No. 4, 19 (2003).
3. G. B. Fershtater, A. Gerdes, and V. N. Smirnov, *Age and History of the Formation of the Adui Granite Massif*, in *Yearbook-2001* (Inst. Geol. Geokhim., Yekaterinburg, 2003), pp. 146–150 [in Russian].
4. A. A. Krasnobaev, F. Bea, G. B. Fershtater, et al., in *Geology and Metallogeny of Ultramafic–Mafic and Granitoid Intrusive Associations in Fold Zones* (Inst. Geol. Geokhim., Yekaterinburg, 2004), pp. 345–350 [in Russian].